INTERFACE TO INTERFACE CORE CRACKS IN SANDWICH STRUCTURES

Jens H Andreasen*, Johnny Jakobsen*, Anders Lyckegaard **
***Department of Mechanical Engineering, Aalborg University, Denmark**
****NKT Flexibles I/S, Brøndby, Denmark**

Keywords: *Sandwich Structures, Fracture Mechanics*

Abstract

The interface to interface crack in a sandwich construction is investigated. The crack constitutes a transition state between the core crack and the interface crack. Furthermore the crack problem can be used to assess the tunneling of cracks through a sandwich structure.

The crack is analyzed within the framework of analytical elasticity. Though central parts of the solution have to be established numerically, the analytic parts give useful insight into the nature of the solution, especially pertaining to the nature of the singular or near tip behavior of the crack. During the course of analyzing this problem it is established that for a wide variety of problems two singularity parameters have to be carried through in order to attain accurate solutions.

Results are given in terms of a case study pertaining to sandwich constructions with aluminum faces and two different foamed PVC core, as well as in more generalized terms.

1 Introduction

Sandwich structures are widely used in applications where a combination of large stiffness and low weight are of great importance. The layered structure of the sandwich construction with stiff face sheets and a soft core material in between is the essential idea behind obtaining high stiffness in combination with low weight. The low stiffness core is, on the other hand, a critical part of the sandwich structure, as the desire for low weight also has a tendency to induce relatively low strength. Among the failure modes for sandwich structures are core cracking for cores with relatively poor toughness.

In this investigation a core to core crack configuration is presented. In static and fatigue loading [1,2] of sandwich structures failure by cracking of the core often starts by small cracks in the core center which grows towards the interfaces between the core and the face sheets. As the cracks approach the interfaces the influence of the very stiff face sheets as compared to the core becomes increasingly important. Detailed information about the transition from a core crack to an interface crack requires the interface touching crack solution, which is addressed in this paper. The solution is furthermore applied to asses the ability of such cracks to tunnel through the sandwich structure.

The light weight properties are obtained through the lay-up of the sandwich structure it self, which in its basic structure consists of two strong and stiff face sheets with a light weight and relatively soft core in between. The face sheet material can be eg. steel, aluminum or a fiber reinforced polymer. The core material can be eg. a polymeric foam, balsa wood or a honeycomb structure. In either case a very large stiffness difference between the face sheet material and the core material is present. The general properties of sandwich structures have been described in text books such as [3] and [4]. In this study emphasis is put on a sandwich construction with aluminum faces and foamed PVC cores.

In this analysis the interface to interface crack is addressed through an analytical approach for solving the appropriate linear elastic equations.

2 Teory

2.1 Geometrical Configuration

The sandwich structure under investigation is depicted in Fig. 1. The sandwich consists of two face sheets and a core in a symmetric lay-up with a collected thickness 2h, and a core thickness of 2t. A crack of length 2c the face sheets and the core are assumed isotropic with Young's moduli E_1 and E_2 and Poisson's ratios ν_1 and ν_2 respectively. The far

field loading is any combination of tension *P*, bending *M* or shear *V*.

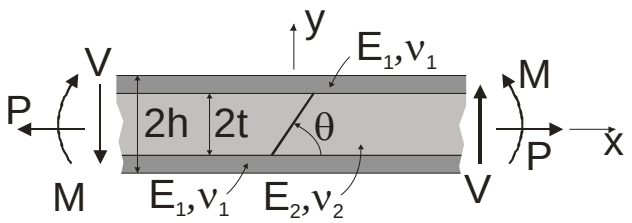

Fig. 1. An interface to interface crack in a sandwich structure

Within the same framework the ability of an interface to interface crack to tunnel through the sandwich structure can be determined. A tunnel crack is depicted in fig. 2., where the crack has partially penetrated the sandwich. The analysis of such a tunneling crack consists of estimating the change in strain energy density ahead of the crack, and well behind the crack front, or more directly estimating the work per unit thickness needed to close the crack.

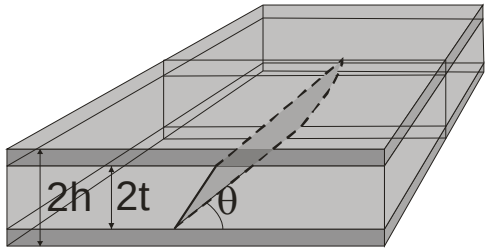

Fig. 2. Tunneling of a crack in a sandwich.

2.2 Crack Modelling

The crack is modeled by the dislocation pile-up method [5]. Such that the crack opening is obtained through integral equations which ensure that the traction boundary conditions along the crack faces are satisfied.

Formally this can be written as

$$\sigma_{\theta\theta} + i\sigma_{r\theta}\big|_{z\in C} = \int_C B(\eta)K(z,\eta)d\eta \qquad (1)$$

where C is the domain of the crack, $B(\eta)$ is the dislocation pile-up corresponding to Burgers vector between η and η+dη. $K(z,\eta)$ is correspondingly the influence function for a dislocation [6]. In the analysis of the influence function due consideration to the large difference in stiffness between the core and face sheet materials has to be taken into account. This involves explicit extraction of near singular terms appearing due to the weak coupling between the face sheets through the core.

The dislocation pile-up is most can be separated into terms as

$$B(\eta) = B_0(\eta) + k_{U1}\frac{L+\eta}{(L-\eta)^{\lambda_1}} + k_{U2}\frac{L+\eta}{(L-\eta)^{\lambda_2}} + k_{L1}\frac{L-\eta}{(L+\eta)^{\lambda_1}} + k_{L2}\frac{L-\eta}{(L+\eta)^{\lambda_2}} \qquad (2)$$

Where $L=t/\sin(\theta)$. $B(\eta)$ is in general complex.

$B_0(\eta)$ is non-singular and the terms including k_{U1} and k_{U1} pertains to the upper crack tip and k_{L1} and k_{L2} pertains to lower crack tip at respectively. The singularity parameters λ_1 and λ_2 can be obtained through potential analyses [7] or in the process of solving (1). When the crack is moderately slanted two singularity parameters appear, and for strongly slanted cracks the singularity parameters becomes complex. The appearance of two singularity parameters makes the basic description of the dislocation pile-up somewhat more involved compared to the vertical crack, where only one singularity parameter appears. It should be emphasized that both parameters should be explicitly included in order to obtain accurate numerical results.

The separation of the dislocation density function (2) into a sum rather than the more conventional product of functions containing the appropriate singularities offer the advantage that the choice of integration scheme is much freer. Furthermore analytical integration can be applied to a number of details in the kernel and dislocation density function, whereby the remaining numerical integrations can be made quite robust. The latter has been applied extensively in the numerical implementation of the present problem.

The ability of the crack to tunnel through the sandwich structure can be described through the average energy release rate $\underline{G}$ along front of a tunneling crack as depicted in fig. 2. The calculation of the energy release rate is most conveniently done by determining the work per unit thickness needed to close the crack given by

$$\underline{G} = \frac{1}{4L}\int_C \mathrm{Re}\{(\sigma_{\theta\theta} + i\sigma_{r\theta})(\delta_\theta + i\delta_r)\}d\eta \qquad (3)$$

where $\sigma_{\theta\theta}$+$i\sigma_{r\theta}$ are the stresses determined far ahead of the crack, ie. the rather trivial solution for a sandwich without a crack. The term δ_θ+$i\delta_r$ is the crack opening given in terms of the dislocation density function by

$$(\delta_\theta + i\delta_r)\big|_\eta = \int_{-L}^{\eta} B(\tau)d\tau \qquad (4)$$

An outline of the analysis method for the end-point singular solution is given in the following. As well as the resulting tunneling crack results.

2.3 Determination of kernel function

The kernel function is established using Muskhelishvili's potentials [7] for a dislocation in the core material of the sandwich.

Stresses are obtained in terms of Muskhelishvili's potentials as

$$\begin{aligned}\sigma_{rr}+\sigma_{\theta\theta} &= 2\left[\Phi(z)+\overline{\Phi(z)}\right]\\ \sigma_{\theta\theta}-\sigma_{rr}+2i\sigma_{r\theta} &= 2\left[\bar{z}\Phi'(z)+\Psi(z)\right]e^{2i\theta}\end{aligned} \tag{5}$$

and displacements are given by

$$2\mu\,(u_x+iu_y)=\kappa\varphi(z)-z\overline{\phi'(z)}-\overline{\psi(z)} \tag{6}$$

where

$$\begin{aligned}\Phi(z)&=\phi'(z)\\ \Psi(z)&=\psi'(z)\end{aligned} \tag{7}$$

in accordance with the usual conventions of notation for complex potentials. μ is the shear modulus and κ is the Kolosov constant given by κ=3-4ν for plane strain and κ=(3-ν)/(1+ν) for plane stress respectively.

The displacement derivative

$$2\mu\frac{\partial}{\partial x}(u_x+iu_y)=\mu\Phi(z)-\overline{\Phi(z)}-z\overline{\Phi'(z)}-\overline{\Psi(z)} \tag{8}$$

is applied to formulate displacement continuity across the interfaces. This ensures continuity to within immaterial rigid body translations and offers the advantage, that only potentials pertaining to stresses (5) needs to be determined.

Using the transformation relations

$$\begin{aligned}\Phi(z')&=\Phi(z-z_0)\\ \Psi(z')&=\Psi(z-z_0)-\overline{z}_0\Phi'(z-z_0)\end{aligned} \tag{9}$$

it suffices to solve for a dislocation centered at x=0, and use (9) for off axis dislocations.

The potential for the upper face sheet can be expressed as

$$\begin{aligned}\Phi_1^D(z)&=i\int_0^\infty s\left[a_1(s)\,e^{-isz}+\overline{a_2(s)}\,e^{isz}\right]ds\\ \Psi_1^D(z)&=-2i\int_0^\infty s\left[\left[\left(1-\frac{1}{2}isz\right)a_1(s)+sa_3(s)\right]e^{-isz}\right.\\ &\qquad\left.+\left[\left(1+\frac{1}{2}isz\right)\overline{a_2(s)}+s\overline{a_4(s)}\right]e^{isz}\right]ds\end{aligned} \tag{10}$$

The potential for the core can be written as

$$\begin{aligned}\Phi_2^D(z)&=\Phi_0(z)+i\int_0^\infty s\left[a_5(s)\,e^{-isz}+\overline{a_6(s)}\,e^{isz}\right]ds\\ \Psi_2^D(z)&=\Psi_0(z)-2i\int_0^\infty s\left[\left[\left(1-\frac{1}{2}isz\right)a_5(s)+sa_7(s)\right]e^{-isz}\right.\\ &\qquad\left.+\left[\left(1+\frac{1}{2}isz\right)\overline{a_6(s)}+s\overline{a_8(s)}\right]e^{isz}\right]ds\end{aligned} \tag{11}$$

where $\Phi_0(z)$ and $\Psi_0(z)$ pertains to a dislocation in an infinite medium of core material, as given below.

The potentials for the lower face sheet are expressed as

$$\begin{aligned}\Phi_3^D(z)&=i\int_0^\infty s\left[a_9(s)\,e^{-isz}+\overline{a_{10}(s)}\,e^{isz}\right]ds\\ \Psi_3^D(z)&=-2i\int_0^\infty s\left[\left[\left(1-\frac{1}{2}isz\right)a_9(s)+sa_{11}(s)\right]e^{-isz}\right.\\ &\qquad\left.+\left[\left(1+\frac{1}{2}isz\right)\overline{a_{10}(s)}+s\overline{a_{12}(s)}\right]e^{isz}\right]ds\end{aligned} \tag{12}$$

The potential for a dislocation in an infinite medium can be determines as

$$\begin{aligned}\Phi_0^D(z)&=i\int_0^\infty s\left[b_1(s)\,e^{-isz}+\overline{b_2(s)}\,e^{isz}\right]ds\\ \Psi_0^D(z)&=-2i\int_0^\infty s\left[\left[\left(1-\frac{1}{2}isz\right)b_1(s)+sb_3(s)\right]e^{-isz}\right.\\ &\qquad\left.+\left[\left(1+\frac{1}{2}isz\right)\overline{b_2(s)}+s\overline{b_4(s)}\right]e^{isz}\right]ds\end{aligned} \tag{13}$$

For a dislocation at y_0 (and x_0=0) the functions $b_1(s)$ through $b_4(s)$ in (13) are given by

$$\begin{aligned}&y>y_0:\\ &b_1(s)=Ae^{-sy_0}/s,\\ &b_2(s)=0,\\ &b_3(s)=-\left((1+2sy_0)A+\overline{A}\right)e^{-sy_0}/(2s^2),\\ &b_4(s)=0\end{aligned} \tag{14}$$

and

$$\begin{aligned}&y<y_0:\\ &b_1(s)=0,\\ &b_2(s)=-\overline{A}e^{sy_0}/s,\\ &b_3(s)=0,\\ &b_4(s)=-\left((1-2sy_0)\overline{A}+A\right)e^{sy_0}/(2s^2)\end{aligned} \tag{15}$$

for y above y_0 and below y_0 respectively. The parameter A is given as

$$A=i\frac{(b_x+ib_y)\mu_2}{\pi(1+\kappa_2)} \tag{16}$$

where b_x and b_y are the x and y components of Burgers vector. Index 2 refers to the core material in accordance with fig. 1.

The formulation followed in (10) through (13) constitutes a Fourier transform formulation of

Muskhelishvili's potentials. The truncated Fourier transforms with integration limits of 0 to ∞ rather than the usual $-\infty$ to ∞ is allowed by solving for a dislocation situated at x_0=0, and utilizing the transformation formula (9) for generalizing to off axis solutions rather than the Fourier transform formulation it self.

Applying traction continuity through (5) and displacement continuity through (8) for the interfaces between the core and the upper and lower face sheets of the sandwich yields 8 equations for determining the functions a_1(s) through a_{12}(s) in (10)-(12). The traction free outer surface for the upper and lower face sheets renders the remaining 4 equations. The 12 equations for the boundary conditions are reduced to algebraic equations in a_1(s)…a_{12}(s) by removing the integrations introduced in (10)-(13) such that the equations are satisfied by matching the integrands appropriately.

The determination of the functions a_1(s)…a_{12}(s) is straight forward but explicit expressions are forbiddingly large, and the integrations in (10)-(12) consequently have to be determined numerically. A Gauss-Laguerre quadrature was employed for this task. In order to obtain stable numerical integration it is necessary to remove singular and often certain near singular terms in a_1(s)…a_{12}(s) and perform analytical integrations on these numerically unstable parts. The first appears in general for far field terms. The latter particularly appears for large stiffness differences between the core and face materials.

2.4 Near tip analysis in the core material

In order to assess the nature of the solution it is necessary to investigate the potentials for the core material. In general the potentials can be written as

$$\begin{aligned}\Phi_2(z) &= \int_C \Phi_2^D(z, z_0)\,d\eta \\ \Psi_2(z) &= \int_C \Psi_2^D(z, z_0)\,d\eta\end{aligned} \tag{17}$$

where $\Phi_2^D(z,z_0)$ and $\Psi_2^D(z,z_0)$ are the obtained from (10) to (13) such that z_0 is on the crack C with natural coordinate η and the dislocation density is adjusted such that the traction free crack faces is ensured. The excact integration of (17) is of course a numerical problem, but partly analytical integration greatly improves the solution stability, as well as giving qualitative insight into the solution structure.

The potentials (17) for the core material can be integrated partly for Cauchy singular terms and the associated image terms due to the interfaces along with the power law terms in the dislocation density function (2). Formally (17) be rewritten as

$$\begin{aligned}\Phi_2(z) = \Phi_0(z) &+ \frac{L(z,k_{U1},\lambda_1)}{\left(L-\frac{z}{\varsigma}\right)^{\lambda_1}} + \frac{L(z,k_{U2},\lambda_2)}{\left(L-\frac{z}{\varsigma}\right)^{\lambda_2}} \\ &+ \frac{L(z,k_{L1},\lambda_1)}{\left(L+\frac{z}{\varsigma}\right)^{\lambda_1}} + \frac{L(z,k_{L2},\lambda_2)}{\left(L+\frac{z}{\varsigma}\right)^{\lambda_2}}\end{aligned} \tag{18}$$

$$\begin{aligned}\Psi_2(z) = \Psi_0(z) &+ \frac{M(z,k_{U1},\lambda_1)}{\left(L-\frac{z}{\varsigma}\right)^{\lambda_1}} + \frac{M(z,k_{U2},\lambda_2)}{\left(L-\frac{z}{\varsigma}\right)^{\lambda_2}} \\ &+ \frac{M(z,k_{L1},\lambda_1)}{\left(L+\frac{z}{\varsigma}\right)^{\lambda_1}} + \frac{M(z,k_{L2},\lambda_2)}{\left(L+\frac{z}{\varsigma}\right)^{\lambda_2}}\end{aligned} \tag{19}$$

where $\phi_2(z)$ and $\psi_2(z)$ are nonsingular functions. $L(z,k,\lambda)$ and $M(z,k,\lambda)$ are given by

$$\begin{aligned}L(z,k,\lambda) &= k\left(\frac{z}{\varsigma}+L\right)\left(\cot(\lambda\pi)-i\xi\right) \\ &+\left(k+2i\frac{t}{L}\left(k-(2-\lambda)\bar{k}\right)\left((2-2it)\varsigma+4it\varsigma\bar{k}\right)\right)* \\ &*\left(\cot(\lambda\pi)+i\right)e^{-2i\lambda\theta}\delta_1\frac{1-\delta_2}{1-\delta_2}\end{aligned}$$

$$\begin{aligned}M(z,k,\lambda) &= \left(\left(\bar{k}(z-2it)\varsigma+L\right)\frac{1-\delta_1}{1-\delta_2}\right. \\ &-\left(\left(2i\frac{(2it-z)(2-\lambda)\varsigma}{L}+1\right)t\bar{k}\right. \\ &-\left(\left((2it-z)\varsigma-L\right)(2-\lambda)+(1+\lambda)L+\frac{2\lambda L^2}{(z-2it)\varsigma-L}\right)* \\ &*\left(k-2i(1-\lambda)\frac{t}{L\varsigma}\bar{k}\right)\varsigma\left.\delta_1\frac{1-\delta_2}{1-\delta_1}\right)\left(\cot(\lambda\pi)+1\right)e^{-2i\lambda\theta} \\ &-\frac{1}{\varsigma^2}\left(\left(\frac{z}{\varsigma}+L\right)\left((2-\lambda)k-\bar{k}\right)-\left(1+\lambda+\frac{2\lambda L}{\frac{z}{\varsigma}-L}\right)Lk\right)* \\ &*\left(\cot(\lambda\pi)+\xi\right)\end{aligned} \tag{20}$$

where $\varsigma = e^{i\theta}$ and ξ is 1 for z to the right of the crack and -1 for z to the left of the crack. δ_1 and δ_1 are given by

$$\begin{aligned}\delta_1 &= \frac{\alpha-\beta}{1-\beta} \\ \delta_2 &= \frac{\alpha+\beta}{1+\beta}\end{aligned} \tag{21}$$

and α and β are the Dundurs parameters [8] given by

$$\alpha = \frac{\mu_1(1+\kappa_2)-\mu_2(1+\kappa_1)}{\mu_1(1+\kappa_2)+\mu_2(1+\kappa_1)} \qquad (22)$$
$$\beta = \frac{\mu_1(1-\kappa_2)-\mu_2(1-\kappa_1)}{\mu_1(1+\kappa_2)+\mu_2(1+\kappa_1)}$$

The traction along the crack face due to the singular endpoints can be obtained from (18) to (20) by neglecting the non-singular parts of the potentials. For the traction to be finite as the crack tips are approached the following equations are obtained

$$0 = Q_1\overline{Q_1} - Q_2\overline{Q_2} \qquad (23)$$

where

$$Q_1 = 4i(1-\lambda)(e^{2i\theta}-1)\sin((1-\lambda)(2\theta-\pi))\delta_1\frac{1-\delta_2}{1-\delta_2} \qquad (24)$$

$$Q_2 = 4\cos(\lambda\pi) - 2e^{(1-\lambda)(2\theta-\pi)i}\delta_2\frac{1-\delta_1}{1-\delta_2}$$
$$+(8(1-\lambda)^2\sin^2(\theta)e^{(1-\lambda)(2\theta-\pi)i} - 2e^{-(1-\lambda)(2\theta-\pi)i})\delta_1\frac{1-\delta_2}{1-\delta_1}$$

such that (23) constitutes a characteristic equation for determining the singularity parameter λ. The characteristic equation (23) is in accordance with that obtained by Zak and Williams[9] by direct application of potential solutions. For a vertical crack equation (23) has a double root. For not too slant cracks (23) has two distinct roots between 0 and 1, and for very slant cracks the roots are complex with a real part less than 1/2.

In the case of two distinct roots an associated phase angle is given by

$$\gamma = \arctan\left(\frac{1}{2}\frac{|Q_1+Q_2|}{\mathrm{Im}(Q_1Q_2)}\right) \qquad (25)$$

The interpretation of the phase angle γ is, that the geometrical singularity parameters in (2) are to interpreted as

$$k_{U1} = c_1 e^{i\gamma_1}$$
$$k_{U2} = c_2 e^{i\gamma_2} \qquad (26)$$

where c_1 and c_2 are real arbitrary numbers determined in the process of solving (1).

3 Results

3.1 Case Studies

Material	H60	H200	Al
E-modulus [Mpa]	60	235	71820
Poisson's ratio	0.31	0.36	0.33
Thickness [mm]	20	20	10

Table 1. Properties for two core materials and the face sheet.

A combination of materials consisting of two PVC core foams and aluminum face sheets of practical use is considered. The elastic properties are given in table 1. along with practically relevant thicknesses of the core and face sheet materials.

The stiff core H200 with aluminum faces will be referred to as case 1 and the softer core material H60 with aluminum faces will be referred to as case 2.

The singularity parameters as obtained from (23) pertaining to case 1 and 2 are illustrated in Fig. 3.

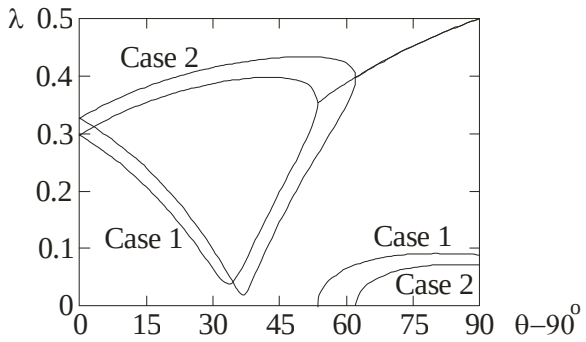

Fig. 3. Singularity parameter λ.

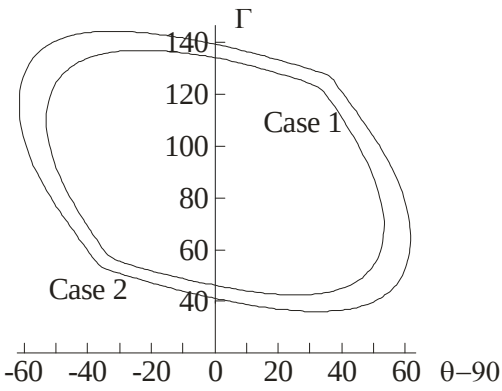

Fig 4. Phase angle for real singularity parameters.

The solution of the characteristic equation (25) gives for the vertical crack (θ-90°=0) a double root of λ =0.3267 and λ =0.2968 for case 1 and case 2 respectively. For a not too slanted crack two distinct real roots appear. For case 1 this regime is limited up to the angle 53.5° and for case 2 up to 62.1°. Above these limits for very slanted cracks the singularity parameter becomes complex. In fig. 3 the upper branches correspond to the real parts of the singularity parameters, whereas the curves at the lower right corner of the figure are the imaginary

parts of the complex singularity parameter. For the interface crack (θ-90°=90) the real part of the singularity parameter approaches ½.

The phase angle associated with real roots as given by (25) corresponding to fig. 3 is shown in fig. 4.

The basic fracture mechanical result for a vertical crack approaching the interface in a sandwich loaded by a tensile force is shown in fig. 5. Relevant solution parameters are listed in table 2. In figure 5 c is the half crack length, such that $c=t$ corresponds to the interface touching crack. The loading is pure tension.

	Case 1	Case 2
α	0.998291	0.993569
β	0.21834	0.27366
$\sigma_c/\underline{\sigma}$	0.000426	0.00159

Table 2. Dundurs parameters and stress carried by the core σ_c normalized by the average stress $\underline{\sigma}$.

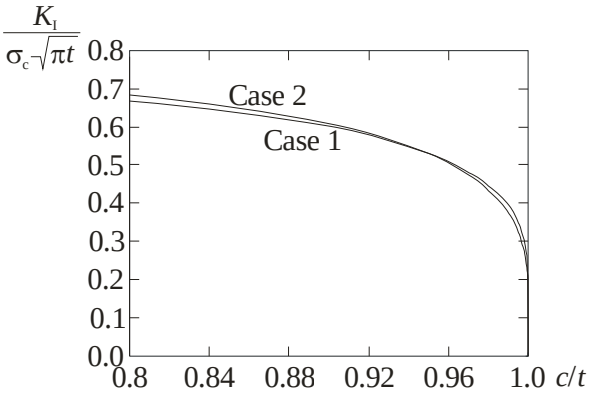

Fig. 6. A symmetrical transverse crack under normal load approaching the interfaces.

In fig. 5. the stress intensity factor K_I is normalized by the core stress in the uncracked configuration σ_c as indicated in table 2. As the crack tips approach the interfaces the SIF's diminishes due to the influence of the stiff face sheets. The singularity parameter in equation 2 is λ =0.2968 and λ =0.3267 for the soft and stiff core materials respectively. In turn the SIF's in fig. 2 diminishes with

$$K_I = A(t-c)^{1/2-\lambda} \qquad (27)$$

where the power ½-λ describes the speed with which the SIF's falls, and the proportionality constant A, obtained as 0.414 for Case 1 and 1.66 for Case 2 respectively.

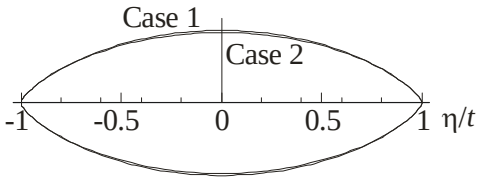

Fig. 7 Crack opening profile for interface to interface crack

The crack opening profile is sketched in figure 7. The opening displacements are very similar, but the stress intensity factors are 0.00131 MPa $m^{0.3267}$/N for case 1 and 0.00573 MPa $m^{0.2968}$/N for case 2 respectively

3.2 General results

The average energy release rate is shown in fig. 8. The thickness of the face sheets is varied with the core kept at a thickness of 10mm. The energy release rates are very close except for very thin face sheets.

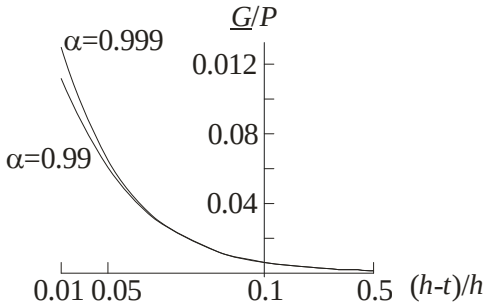

Fig.8 Average energy release $\underline{G}$ rate normalized by force per unit length P for varying thickness of face sheets (β=0.25).

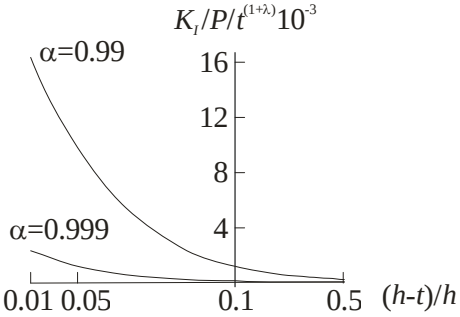

Fig.9 Stress intensity factor normalized by force per unit length P^3) and core thickness to the power 1+λ for varying thickness of face sheets (β=0.25).

Stress intensity factors are depicted in figure 9 for two values of α and β kept at a typical value of 0.25. Increasing the stiffness (or increasing α) clearly

increases the stress intensity factor, and stiffer core materials thereby lead to increased local bending of the face sheets in the vicinity of a crack.

4 Conclusion

An analytical approach to solving the interface to interface crack through the core in a sandwich structure has been devised. From this analysis the generalized stress intensity factors for the interface touching cracks can be determined, and detailed information for cracks approaching the interfaces can be obtained.

The plane strain analysis of the interface to interface crack can further be applied in determining if such cracks are able to tunnel through a sandwich structure. That is the solution provides the necessary information for calculating the energy release rate for crack tunneling.

Interface to interface core cracks can behave in a number of ways depending on the angle of the crack to the interface. It has been demonstrated by example that for slanted cracks two singularity parameters are needed, unless the slanting is large, where a single complex singularity parameter suffices.

References

[1] Burman, M., Zenckert, D., Fatigue of Foam Core Sandwich Beams -1: Undamaged specimens. *Int. J. Fatigue*, **19**, 7, 551-561,1997.

[2] Burman, M., Zenckert, D., Fatigue of Foam Core Sandwich Beams -2: Effect of Initial Damage. *Int. J. Fatigue*, **19**, 7, 563-578,1997.

[3] Zenckert, D., "*An Introduction to Sandwich Structures*". Chamelion Press Ltd.. London, 1995.

[4] Allen, H. G., "*Analysis and Design of Structural Sandwich Pane*l", Pergamon Press, 1969.

[5] Bilby, B. A. and Eshelby, J. D. "Dislocation Theory of Fracture" in "*Fracture*" no. 1, Liebowitz (ed.), Academic Press 1968.

[6] Andreasen, J. H. and Lyckegaard, A. "Analysis of a Sandwich Panel Containing a Transverse Core Crack under In-Plane Loading. Proceedings of ECCM 12, eds. Lamon, J, and Marques, A. T., 2006.

[7] Muskhelishvili, N. I., "*Some Basic Problems of the Mathematical Theory of Elasticity*". Noordhoff, Groningen 1953.

[8] Dundurs, J., Edge-Bonded Dissimilar Orthogonal Elastic Wedges Under Normal and Shear Loading*., J. Appl. Mech.*, sep. pp 650-652, 1969.

[9] Zak, A. R., Williams M. L., Crack Point Singularities at a Bimaterial Interface" *Journal of Applied Mechanics*, **30**, 142-143, 1963.

[10] Romeo, A, Ballarini, R., A Crack Very Close to a Bimaterial Interface. J. Appl. Mech, 62, pp 614-619,1995.